Propagation measurements using array signal processing

S. Catreux, S. Burfoot, P.F. Driessen, R.L. Kirlin
Department of Electrical and Computer Engineering
University of Victoria
P.O. Box 3055, Victoria, B.C., V8W 3P6 Canada

ABSTRACT: Propagation measurements using a synthetic aperture array may be used to determine direction of arrival as well as delay of multipath components. The measurement data may then be used to validate ray-tracing propagation models, as well as to evaluate smart antenna array processing techniques.

In this paper, we investigate the limitations of the synthetic aperture measurement technique, in particular, we consider both linear and cross arrays, and determine the corresponding positioning accuracy required. Thus we present both simulated and experimental results of complex impulse responses at 1 Ghz, using a synthetic aperture array, taken in several typical scenarios, using both linear array and cross-array processing.

We find that the positioning error must be less than 5% for a half-wavelength spaced linear array to ensure that 90 percent of spurious responses are more than 30 dB down relative to the source signal.

I. INTRODUCTION

Our overall objective is to obtain cell site coverage maps which includes the multipath delay profile as well as the signal strength, using data bases of terrain and nearby buildings. Such coverage maps may be used to predict the signal quality (bit error rate) or outage probability as a function of receiver location for digital cellular radio systems. The best cell layout may thus be determined by computer experiment rather than actual measurements.

The first step towards this objective may be achieved by using a scattering model to establish a reflection coefficient to each surface element in the building data base, and tracing all rays from transmitter via each such element to receiver. The reflection coefficient will depend on the angles of incidence and reflection, surface roughness and other parameters of the surface element, and may be characterized statistically [1][2] [3]. The second step is to validate this model by comparing its prediction to the measurement result. Thus, to test the accuracy of the coefficients used in these models, measured complex impulse responses at 910 MHz in an urban environment are processed as data from a synthetic aperture array, thus identifying the power reflected at various bearings and distances from the receiver. Thus we assign a reflection coefficient and corresponding intensity to each building wall in the building data base. A plot of the environment as seen from the receiver shows a "radio eyes" (bistatic radar) view of the buildings.

The objective of this paper is to quantify the limitations of the synthetic aperture measurement technique with respect to the positioning error and signal-to-noise ratio. We first describe the experimental setup and data acquisition, followed by a review of the array processing, simulation and measurement results.

II. EXPERIMENTAL SETUP AND DATA ACQUISITION

The impulse response data was recorded at 30 and 60 locations forming a linear or crossed synthetic aperture array, with inter-element spacing of 6 inches (slightly less than a half wavelength at 910 MHz), using a 10 Mb/sec BPSK transmitter with 1023 bit PRBS and sliding correlator receiver, thereby yielding complex impulse responses for the multipath channel with time resolution of one-half chip period or 50 nsec.

The measurements were done on the roof of the Engineeering Lab Wing at the University of Victoria, both for LOS and non-LOS environments. There were two sets of data collected. While the transmitter site was fixed, one set of data was taken from the receiver array along the North to South direction and another collected from along the East to West direction. Each impulse response was measured 8 times, and the average data was then used to determine the DOA spectral information. The data has been first separately processed as from two separate linear arrays according to their orientation, and then jointly processed as one cross-array data. Processing is done using MATLAB on a Pentium 200.

III. ARRAY PROCESSING REVIEW

The array data is processed using minimum variance distortionless response (MVDR, also referred to as Linear

0-7803-3905-3/97/$10.00

Constrained Minimum Variance (LCMV)) as described in [6] [4]. Details of the cross-array signal processing are given in [4][5]. The time window size is set to correspond to the width of the impulse (200 nsec) and spatial smoothing is applied to overcome the coherent multipath problem [7]. The LCMV angle versus distance results are converted into distance versus distance results plots to better coordinate the actual points of reflection with the building data.

To review, consider an uniform linear array composed of M sensors. For simplicity, we assume that the transmitter, the reflected waves and the sensors are located in the same plane and that the impinging waves are in the far-field of the array [4]. Let $\mathbf{x}$ be the $M * 1$ vector received by the array and $\mathbf{a}(\theta)$ be the $M * 1$ "steering vector" of the array towards the direction θ.

The output of the minimum variance beamformer is given by [5] $\mathbf{w}^H\mathbf{x}(t)$ where the weight vector $\mathbf{w}$ is determined by minimizing the output power subject to the constraint of unity gain in the direction θ_1 of the desired signal $\mathbf{w}^H\mathbf{a}(\theta_1) = 1$. Thus

$$\mathbf{w} = \frac{1}{\mathbf{a_1}^H\mathbf{R}^{-1}\mathbf{a_1}}\mathbf{R}^{-1}\mathbf{a_1} \tag{1}$$

where $\mathbf{a_1}$ stands for $\mathbf{a}(\theta_1)$ and $\mathbf{R}$ denotes the sample-covariance matrix computed from m samples of $\mathbf{x}(t)$ at time instants $t_1, \cdots, t_m$. The MVDR power spectrum is given by

$$\mathbf{S_{MVDR}}(\theta) = \frac{1}{\mathbf{a}(\theta)^H\mathbf{R}^{-1}\mathbf{a}(\theta)} \tag{2}$$

MVDR processing for the cross-array is identical, except that the steering vector $\mathbf{a_1}$ is modified to include the elements of both (perpendicular) linear arrays [5].

Spatial Smoothing for the Cross-Array

Spatial smoothing is a preprocessing technique to assist in the estimation of directions of arrival (DOA) of coherent signals [7]. Spatial smoothing starts by dividing a uniform linear array with M sensors into overlapping subarrays of size M_s, with sensors $(1, 2, \cdots, M_s)$ forming the first subarray, sensor $(2, 3, \cdots, M_s + 1)$ forming the second subarray, etc. up to the last subarray forming by $(M - M_s + 1, M - M_s + 2, \cdots, M)$.

Similar to the linear array we can divide a cross array into many overlapping subcross-arrays. Where the EW sensor $1, 2, \cdots, N_s$ and the NS sensor $1, 2, \cdots, M_s$ form the first subcross-array, the EW sensor $2, 3, \cdots, N_s + 1$ and the NS sensor $2, 3 \cdots, M_s + 1$ form the second subcross-array. But then before calculating each estimated subcross-array covariance matrix, we apply an appropriate phase shift on each subarray vector, so that all the subarrays are equivalent and have the same orientation as the subarray centered at the original cross-array, chosen as the reference [8]. In other words, we apply an appropriate phase shift to each sensor EW and NS of each subcross-array,so that the sensors at the center of the sublinear-array NS and the sublinear-array EW composing the subcross-array have a phase difference equal to zero.

Let x_l denote the output of the lth subarray for $l = 1, 2, \cdots, L$, after the phase correction. The covariance matrix of the lth subarray is given by

$$R_l = E[x_l x_l^H]$$

Define the spatial smoothing covariance R_S as the average value of the subarray covariance matrices,

$$R_s = \frac{1}{L}\Sigma_{l=1}^{L} R_l \tag{3}$$

The smoothing process effectively decorrelates the coherent multipath signal arrivals, rendering the methods of solution for incoherent signals effective.

IV. RESULTS AND DISCUSSIONS

Simulation

To verify the array processing and to determine the positioning accuracy requirements, simulated data was generated in the same file format as the measured data, and then processed. Results for three sources at compass bearings of 0, -50 and -100 degrees with relative powers of 0, -3 and -20 dB and delays 25, 30, 33 time samples (25 nsec per time sample) are shown in Figures 1a,b in terms of apparent source location (bearing and distance) relative to the receiver. In this example, the SNR [1] is 20 dB and the positioning error is zero. For linear array processing, there is symmetry (ambiguity) about the array axis for both the NS and EW arrays. For cross-array processing, the ambiguity is removed (Figure 1c), the 3 signals are represented by the 3 dark spots on the plot.

Different subarray sizes M_s

Consider q coherent wavefronts to be detected by a linear array of M sensors. The number of subarrays is then equal to $M - M_s + 1$. We recall that the modified covariance matrix of the signals will become non-singular by spatial smoothing if $q + 1 <= M_s <= M - q + 1$. The larger M_s, the smaller the 'noise floor' in the image, because the array gain is larger. On the other hand, when M_s becomes smaller, the number of subarrays increases, and the decorrelation of the signals is better achieved. Therefore, there is a tradeoff and the best value for M_s is found to be half the effective aperture. Figures 1abc were calculated with a subarray of length 17. With a subarray of 5, the noise floor increases, whereas with a subarray of

[1] We define the output SNR (after correlation) of the impulse responses as $1/\sigma^2 B$, where the amplitude of the largest correlation peak is normalized to 1, and $\sigma^2 B$ is the noise power with $B = 1$ Khz (sliding correlator offset).

25, insufficient decorrelation leads to perturbations in the power estimation. The graphical results are omitted here due to the limitations of the grey scale representation, but will be presented at the conference.

Effect of SNR and positioning errors

We assume that the positioning error is gaussian with a standard deviation σ_p normalized as a fraction of the half-wavelength interelement spacing. We find that good DOA results are obtained even for SNR $\rho = 1$ (0 dB). The noise floor in the image is found to be about 15 dB less than the SNR, as expected due to the subarray gain. The weakest signal at -20 dB is lost in the noise.

Defining $n(t, \sigma_p, \rho)$ as the number of pixels above a given threshold t, we quantify the spurious response as $S = n(t, \sigma_p, \rho) - n(t, 0, \infty)$ normalized by the total number of pixels. The positioning error is expressed as the ratio $e = 3\sigma_p/(\lambda/2)$. Figure 2 shows how the spurious responses (extra pixels) increase with positioning error, with an SNR of 20 dB, for a single source. [2]

From Figure 2, we can assess the probability that a given pixel is a real source rather than a spurious response due to positioning error or noise. For example, for a threshold of -30 dB below the strongest source, 8 percent of the pixels will be above this threshold with a positioning error $e = 0.05$, thus the probability that a pixel at -30 dB is a real source is 92 percent. Figure 2 helps to determine an upper bound on the positioning error to achieve a specified dynamic range in the image.

Figure 2 is for the NS array, the EW and cross array results are similar.

Multiple sources in the same time window

The cross array is unable to distinguish the true source from the ambiguity when the sources share the same ambiguities in the linear array processing, and the delays fall in the same time window. Results for 2 sources at compass bearings of -50, 130 degrees with relative powers of 0, -3 dB are shown in Figure 3 with cross array processing. The ambiguities are still there. If these sources arrive at different delays, then the ambiguities are not processed in the same time window, and the DOAs would be resolved.

Measurements

For the measured results we consider first the simple case of one source in LOS. Linear and cross array processing shows qualitatively the same results as in Figure 1. The cross array result (Figure 4) shows spurious responses as expected due to positioning error. Other measurement results with multiple sources will be presented at the conference.

[2] The time window is limited to the pulse width (7 time units) centered around the strongest source at delay 25.

V. SUMMARY

Synthetic aperture techniques can be useful for propagation measurements where angle-of-arrival information is desired. Linear arrays retain a DOA ambiguity symmetrical with the array axis. Cross arrays can resolve this ambiguity with multiple sources provided that the sources are not processed in the same time window (i.e. their distances from the receiver are different by at least the resolution of the measurement system). Thus the results of processing cross array data must be interpreted with care.

References

[1] Braun, W.R. and U. Dersch, "A physical mobile radio channel model", *IEEE Trans. Vehic. Tech.*, vol. 40, No. 2, pp. 472-482, May 1991.

[2] Lebherg, M., W. Wiesbeck and W. Krank, "A versatile wave propagation model for the VHF/UHF range considering three- dimensional terrain", *IEEE Trans. Ant. Prop.*, vol. 40, pp. 1121-1131, 1992.

[3] Beckmann, P. and A. Spizzichino, *The scattering of electromagnetic waves from rough surfaces*, Pergamon Press, 1963.

[4] R.L. Kirlin, P.F. Driessen, "Relationship between measured 900 MHz complex impulse responses and topographical map data", *Proc. IEEE Vehic. Tech. Conf.*, pp. 1811-1815, 1994.

[5] P.F. Driessen, "Propagation measurements using synthetic aperture radar techniques", *IEEE Vehic. Tech. Conf.*, Atlanta, 1996.

[6] S. Haykin, *Adaptive Filter Theory.* Englewood Cliffs, NJ: Prentice-Hall, 1986.

[7] T.J. Shan, M. Wax, T. Kailath, "On Spatial Smoothing for Direction-of-Arrival Estimation of Coherent Signals", *IEEE Trans. Acoust., Speech, Signal Processing*, vol. ASSP-33, pp. 806-811, 1985.

[8] H. Wang, K.J.R. Liu, "Spatial smoothing for arrays with arbitrary geometry", *Proc. IEEE ICASSP*, pp. 509-512.

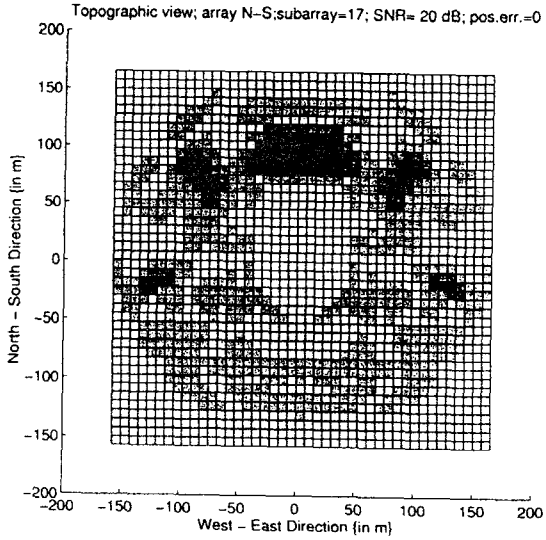

Figure 1a

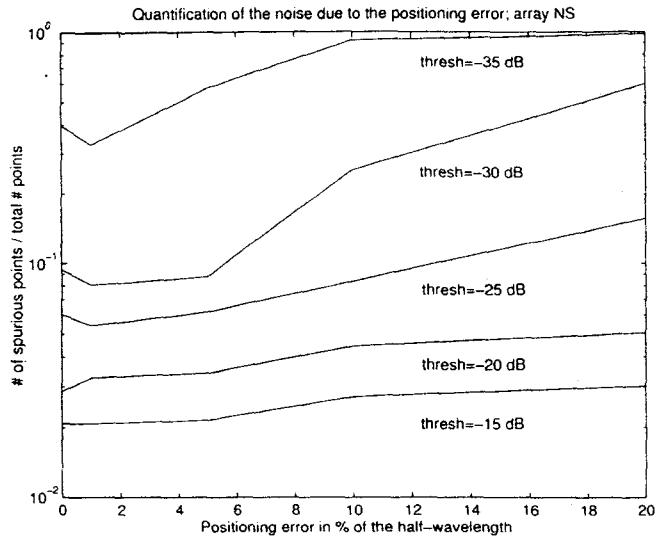

Figure 2

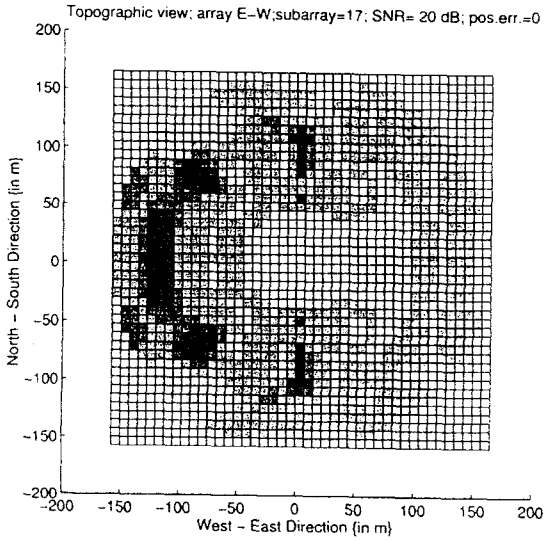

Figure 1b

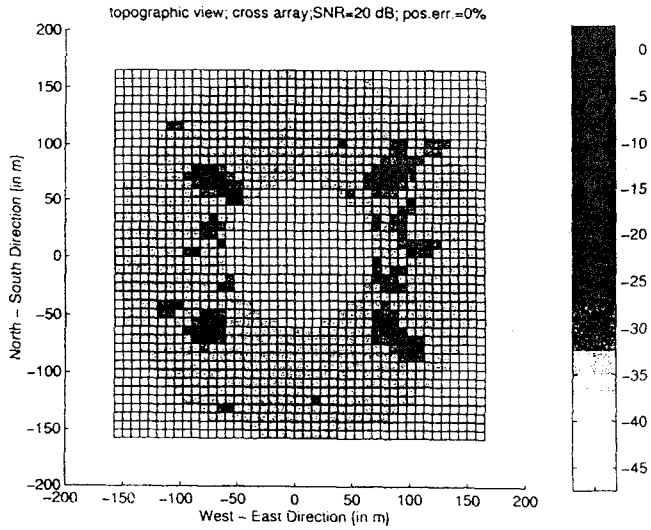

Figure 3

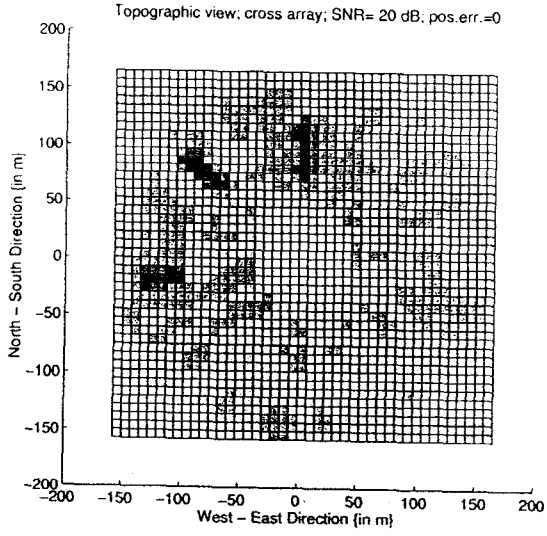

Figure 1c

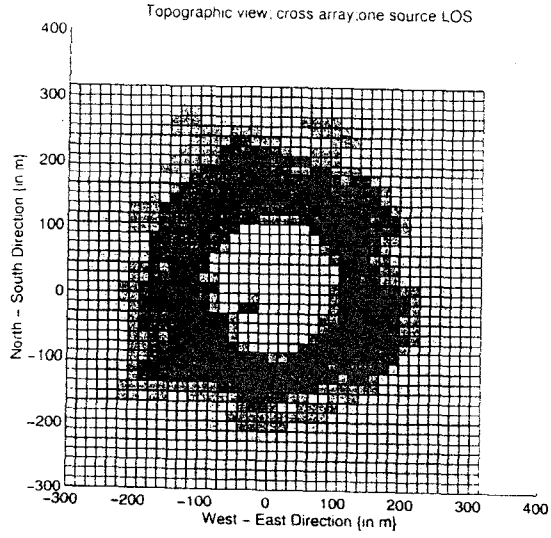

Figure 4